ELSEVIER

Biophysical Chemistry 58 (1996) 313–323

Biophysical Chemistry

A stochastic model for the sigmoidal behaviour of cooperative biological systems

M. Abundo [a,b], L. Accardi [a,b], A. Finazzi Agrò [c], G. Mei [c], N. Rosato [a,c,*]

[a] *Centro Vito Volterra, Università di Roma "Tor Vergata", via di Tor Vergata 135, 00133 Rome, Italy*
[b] *Dipartimento di Matematica, Università di Roma "Tor Vergata", via della Ricerca Scientifica, 00133 Rome, Italy*
[c] *Dipartimento di Medicina Sperimentale e Scienze Biochimiche, Università di Roma "Tor Vergata", via di Tor Vergata 135, 00133 Rome, Italy*

Received 27 March 1995; revised 11 July 1995; accepted 18 July 1995

Abstract

A stochastic model for cooperative transitions in biological systems based on a Markov chain is proposed. This model requires only two parameters, the mean probability, p, and the coupling capacity, Δp, which measure the probability of forming a new weak bond depending on the number of similar bonds already formed and it is also responsible for the transition. In this paper we show how the model works for a large number of identical molecules and how it can be useful for studying the noise around the centre of the transition where, increasing the degree of cooperativity, i.e. the number n in the well-known Hill equation, the width of the noise increases along with its fractal dimension. A simple relationship between the degree of cooperativity and the parameter Δp is proposed, suggesting that the cooperativity of real biological transitions is related to the coupling capacity Δp of the present model.

Keywords: Stochastic model; Markov chain; Cooperativity; Sigmoidal transition; Fractal dimension; Computer simulation

1. Introduction

In a previous paper [1], a stochastic model for cooperative interactions in proteins was proposed. The cooperativity in biological systems involves the concerted formation or rupture of many similar weak chemical bonds. Mathematically, this situation can be described by a Markov chain, which, even depending on two parameters only (the mean probability p and the coupling capacity Δp), offers a surprising wealth of qualitative behaviours when the two parameters are varied.

In our model the probability of forming a new bond depends on the total number of bonds already present in the system: the higher the number of bonds already formed, the greater the probability that additional bonds can be formed, and vice versa.

The aim of the present paper is the application of this mathematical model to the biological systems which undergo transitions following a sigmoidal curve. We point out that the model, which is a stochastic one, appears to improve the qualitative description of the above biological systems, in addition to the more familiar deterministic models. The

* Corresponding author. Tel.: +39-6-72596456, Fax: +39-6-20427292, E-mail: rosato@mat.utovrm.it

SSDI 0301-4622(95)00111-5

advantages of this stochastic model are the following:

- the simplicity of the model;
- the fact that it depends on two parameters only;
- the relatively short simulation time required.

In fact, the model depends on the microscopic parameters p and Δp; the mean probability p is related to $\exp(-\Delta G/RT)$, where ΔG represents the mean activation free energy for the formation of a chemical bond, T is the absolute temperature and R is the Rydberg constant. In this way the parameter p is directly controlled by physical, macroscopic variables such as temperature, pH, etc. On the other hand, the number Δp turns out to express the degree of cooperativity, which is related to the steepness of the sigmoidal curve, as otherwise expressed by the well-known parameter α (see below). Thus, once α, i.e. the slope of the tangent line to the sigmoidal curve at the middle point of the transition, is determined, we can calculate, by our model, the coupling capacity Δp.

More in detail, the cooperative systems are characterized by a sharp transition, indicating that a large variation of the output takes place in a very small interval of the independent variable. Significant examples of these systems are:

- the binding of four oxygen molecules to one haemoglobin molecule [2];
- the thermal transition from gel to sol phase of artificial and natural membranes [3];
- the unfolding of macromolecules like DNA, proteins, etc. [4].

All these phenomena are empirically described by a sigmoidal curve:

$$y = \frac{x^\alpha}{1 + x^\alpha} \qquad (1)$$

where α is related to the cooperativity of the change in y as a function of $x > 0$. Here, x can be considered as a physical state-variable of the system and y the related variable which indicates if, and how, the transition takes places.

When $\alpha = 1$, the transition is non-cooperative, while for $\alpha \to \infty$ (in practice, α being large) the transition is all or none and the total change in y takes place in a very narrow interval of x. Indeed, for α large enough, there are two values, say x_- and x_+, such that the function given in Eq. 1 appears to be approximately zero for $0 \le x < x_-$ and it is approximately 1 for $x > x_+$. Then, we can interpret the situation as follows: if $x > x_+$ the system passes to another state and the transition occurs; if $x < x_-$ the transition does not occur. The nature of this phenomenon is showed particularly in the case when $x_- \approx x_+$, since now a threshold value of x exists, such that below this value a transition never occurs, while above this value a transition does take place. Then, for x varying in a very small interval around the threshold value, two different behaviours can be observed, showing an intrinsic instability of the system as a function of x.

The distribution of the noise of the dependent variable around the midpoint of the sigmoidal transition is described by a very complex function, when the independent variable fluctuates randomly with a Gaussian distribution. The function describing the noise of y is characterized by its tails indicating a non-negligible contribution of extreme values of y. In the present work we also propose an alternative characterization of the y-noise, by measuring its fractal dimension [5]. The use of non-linear mathematical tools for the interpretation of the complex behaviour of biological systems has already been reported in the literature (see e.g. [6–8]).

In a previous paper [1], we have measured the degree of cooperativity by the parameter Δp (coupling capacity). In the present paper we describe the relation between the cooperativity α and the parameter Δp. In this case, we show that the mean value of the state of the system (i.e. the number of bonds present) as a function of the parameter p, just behaves as the sigmoidal curve given by Eq. 1. Experimental data have also been compared with our stochastic model; indeed some sigmoidal curves related to cooperative transitions in biological systems (oxygenation of haemoglobin, helix–coil transition in polylysine, and thermal phase transition in DPPC vesicles) can be approximated well enough by the sigmoidal curves obtained using this model, and the cooperativity parameter Δp can be estimated (see Section 3).

In this paper, at variance with the previous one [1], we take into consideration a population of molecules, so that the parameters p and Δp are not fixed, but fluctuate around the mean values $\bar{p}$ and $\overline{\Delta p}$. In this way, the values $\bar{p}$ and $\overline{\Delta p}$ become

macroscopic parameters, while the fluctuating values p and Δp are the microscopic ones.

The qualitative behaviour of the system has been studied both theoretically and by computer simulation.

2. Model

In this section, we briefly recall the model for cooperative interactions in proteins considered in [1].

A definite number of equivalent particles (in this particular case the chemical groups responsible for the formation of identical weak bonds in the macromolecules) and all possible pairing bonds among the particles of the system are considered. A configuration is defined by a sequence of binary random variables

$$\{\xi_k^{(j)}\}_{k=1,\dots,N}$$

such that

$$\xi_k^{(j)} = +1$$

if the kth pair is linked at the discrete time j,

$$\xi_k^{(j)} = -1$$

otherwise. (Here N is the total number of pairings among the particles.) The evolution of the system, starting from an initial configuration $\xi^{(0)}$, is described in terms of the total energy of the system at time j:

$$S_N(\xi^{(j)}) = \sum_{k=1}^{N} \xi_k^{(j)} \tag{2}$$

All the qualitative features of the model are uniquely determined by the following Ansatz:

$$Pr(\xi_k^{(j+1)} = +1) = p + \frac{\Delta p}{N} S_N(\xi^{(j)}) \tag{3}$$

which means that the probability that the kth bond is formed at time $j+1$ depends linearly on the total relative number of bonds already present (that is, existing at time j). This dependence is completely determined by two parameters which we call p and Δp. The parameter p, which we have called the mean probability, is the probability of forming a bond when the total number of existing bonds is exactly $N/2$, as in this case $S_N(\xi^{(j)}) = 0$. The parameter Δp, which we have called the coupling capacity, is the maximum of the increment of the probability to form a chemical bond for a given p.

These two parameters are supposed to satisfy the coherence conditions:

$$p \pm \Delta p \le 1 \quad p \ge \Delta p \ge 0 \tag{4}$$

which state that all probabilities (Eq. 3) have indeed values between 0 and 1.

Note that from Eq. 3 it follows that the larger is Δp, the faster is the transition in the macromolecule.

For each fixed time j, the random variables $\xi_k^{(j)}$, $k = 1,\dots,N$ are conditionally independent, given a fixed level, say n, of the total energy, and Bernoullian with distribution:

$$Pr(\xi_k^{(j+1)} = +1 | S_N(\xi^{(j)}) = n) = p + \Delta p \frac{n}{N} \tag{5}$$

Introducing the new variables $\eta_k = (1/2)(\xi_k + 1)$ and considering the energy X_j in the new variables η_k at time j:

$$X_j = \sum_{k=1}^{N} \eta_k^{(j)}$$

we obtain that X_j is a Markov chain (MC) with state space $\{0,1,\dots,N\}$ and transition probability given by (see [1])

$$p_{nm} = Pr(X_{j+1} = m | X_j = n)$$
$$= \binom{N}{m} \left[p - \Delta p + 2\frac{\Delta p}{N} n \right]^m$$
$$\times \left[1 - (p - \Delta p) - 2\frac{\Delta p}{N} n \right]^{N-m} \tag{6}$$

When $p > \Delta p \ge 0$ and $p + \Delta p < 1$, the MC is irreducible because $p_{nm} > 0 \ \forall n,m$ (see [1]); so there exists a unique invariant distribution $\{\pi_k\}$, $k = 0,\dots,N$, and the phenomenon of convergence to equilibrium holds, i.e.

$$\lim_{n\to\infty} p_{ik}^{(n)} = \pi_k \ \forall i \in \{0,\dots,N\} \tag{7}$$

where $p_{ik}^{(n)}$ is the probability that the system goes from the state i to the state k in n steps. The probabilities π_k are called stationary probabilities, that is, π_k represents the probability that the process stays at the state k, at equilibrium, i.e. after an infinite time, irrespective of the initial state i.

For large N, by using an heuristic argument based on the law of large numbers, the following asymptotic approximation of the stationary probability can be found (see [1], Eq. 2.28):

$$\pi_k \sim \frac{1}{(1-2\Delta p)^N}\binom{N}{k}(p-\Delta p)^k \times (1-\Delta p-p)^{N-k},\ \Delta p \neq \frac{1}{2} \tag{8}$$

However, for $p = 1/2$, the estimate in Eq. 8 is meaningless, since it gives rise to a binomial distribution with parameter $1/2$, independent of Δp. Moreover, the more p deviates from $1/2$, the better is the agreement between the exact values of π_i and those given by Eq. 8 (see [1]). The convergence to the equilibrium given in Eq. 7 implies the validity of the ergodic theorem. Then, the time average of the state of the system during the time interval $[0,+\infty\rangle$ (which depends on p and Δp) can be calculated by the limit:

$$\bar{X} = E_{p,\Delta p}(X) = \lim_{T\to\infty}\frac{1}{T}\sum_{j=0}^{T} X_j = \sum_{k=0}^{N} k\pi_k \tag{9}$$

Using the estimate from Eq. 8, we obtain for large N:

$$\bar{X} = E_{p,\Delta p}(X) \sim N\frac{p-\Delta p}{1-2\Delta p} \tag{10}$$

The value of $\bar{X}$, obtained by computer simulation, agrees very well with the formula in Eq. 10, also for N not very large (Fig. 1). In Fig. 2a, a typical simulation run of X_t is reported; in Fig. 2b and c, different representations of two trajectories are reported using a $X_j \to X_{j+1}$ graph. In Fig. 1, the computed value of $(1/N)\bar{X}$ is plotted as a function of p, for several increasing values of the parameter Δp, with the constraint $p \in [\Delta p, 1-\Delta p]$, for $N = 100$. It is evident that $y = \bar{X}$ as a function of $x = 2p$ is linear and can be considered a trivial case of a sigmoidal curve.

3. Macroscopic ensemble of protein molecules

In this section we extend the model in order to take into account a large number of protein molecules. All the molecules are assumed to be identical and to undergo the same chemical reaction but each molecule can exist at a slightly different conformation during the reaction. This ensemble can be regarded as a distribution of conformations detectable by experimental techniques (see [9]). We suppose that the folding of each individual protein molecule is occurring by the stochastic evolution described in Section 2.

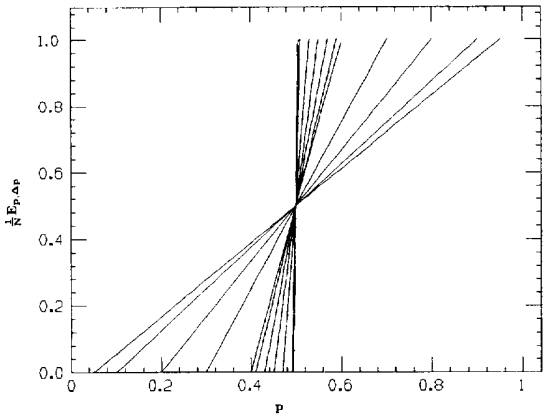

Fig. 1. Plot of the normalized time average $\bar{X} = (1/N)E_{p,\Delta p}(X)$ as a function of p, at increasing values of Δp, from 0 to $1/2$ with the constraint $p \in [\Delta p, 1-\Delta p]$. Here the simulation has been made by using the MC with transition probabilities given by Eq. 7.

Now, we are trying to characterize the evolution of the protein state by means of macroscopic parameters which could be experimentally measured, such as fluorescence lifetime [10,11], as a function of independent experimental variables like temperature, chemicals potentials, or pH. Thus, the microscopic parameters p and Δp are no longer suitable to describe a system consisting of a large number of protein molecules in slightly different states. Indeed, a measurement of a macroscopic parameter is the mean value of that parameter, which is fluctuating around the mean.

We suppose to follow the state of an individual molecule which belongs to a large ensemble of molecules for which the mean value of the parameters, say $\bar{p}$ and $\overline{\Delta p}$, are known. However, the p and Δp values of each molecule can vary according to random variables normally distributed with mean values $\bar{p}$ and $\overline{\Delta p}$, and variance σ^2, σ being a given positive number.

Moreover, we want to remove the constraint (see Eqs. 4 and 5)

$$p \in [\Delta p, 1 - \Delta p] \tag{11}$$

in order that the parameter p as well as Δp can assume the meaning of a physical variable. Generally, we should consider the interval $[0, +\infty\rangle$ as the range of p and Δp. However, for the sake of simplicity, we shall consider the case in which the parameters p and Δp are bounded numbers which can take independently only values in the interval [0,1]. By an obvious change in the scale, we can reduce to the general case of parameters assuming any positive (bounded) value.

Then, recalling the relation of Eq. 3, and denoting

$$q_j = p + \tfrac{\Delta p}{N} S_N\left(\xi^{(j)}\right)$$

we modify it as follows:

$$Pr\left(\xi_k^{(j+1)} = +1\right) = \begin{cases} 0 \text{ if } q_j < 0 \\ q_j \text{ if } q_j \in [0,1] \\ 1 \text{ if } q_j > 1 \end{cases} \tag{12}$$

Now, Eq. 12 is meaningful for any value of p and Δp belonging to the interval [0,1], without any constraint on their values.

Proceeding as done in Section 2, by considering the random variables $\eta_k^{(j)}$, we can construct an MC with state space $\{0,1,\ldots,N\}$ in which the transition probabilities from a state n to another state m are calculated by using Eq. 12 instead of Eq. 3. Now, we are not able to recover the ergodic properties of the MC as in the case in which Eq. 3 holds.

If L is a large integer which denotes the number of molecules of the considered ensemble, for any molecule $i = 1,\ldots,L$, we have computed by numerical simulation of the MC:

$$\overline{X}_i = E_{p,\Delta p_i}(X) = \lim_{T\to\infty} \frac{1}{T} \sum_{t=1}^{T} X_i\ (t)\, i = 1,\ldots,L \tag{13}$$

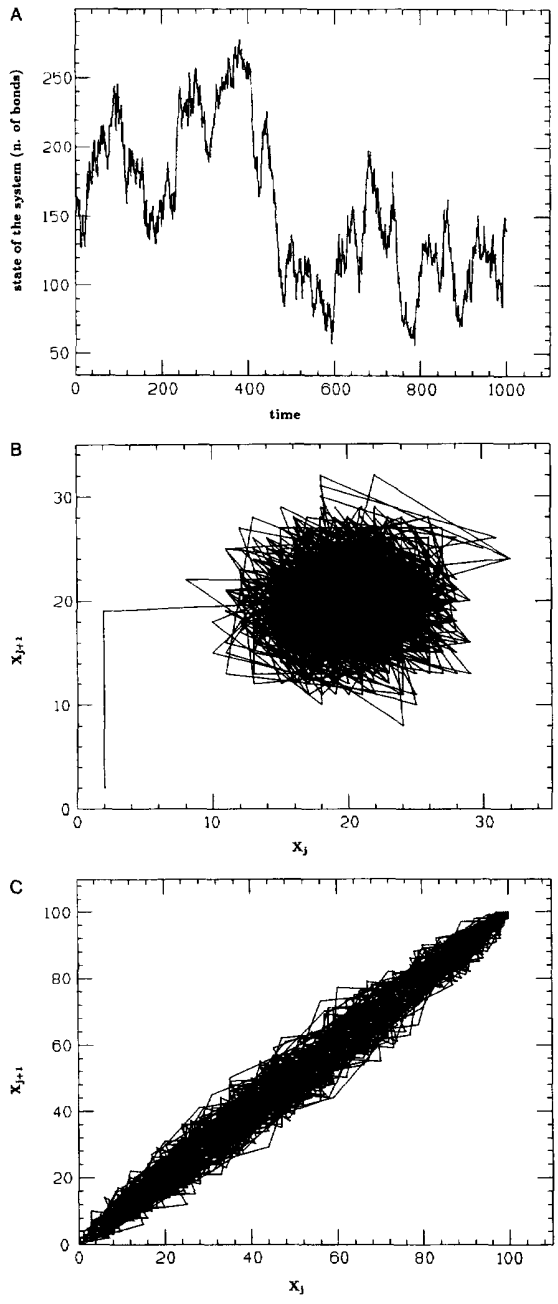

Fig. 2. (A) Plot of the state X_t of the system (vertical axes) versus time (horizontal axes) for $N = 300$, $p = 0.5$, $\Delta p = 0.495$ and $X_0 = 150$ (initial state), obtained by simulating the MC. Obtained from Fig. 1 of [1]. (B) Plot of the state X_{j+1} versus X_j in the case of the MC, for $p = 0.4$, $\Delta p \approx 0$, $N = 50$ and $X_0 = 0$. Note that a shell around the most probable value $X = 20$ is filled up. Obtained from Fig. 8 of [1]. (C) Plot of the state X_{j+1} versus X_j in the case of the MC, for $p = 0.5$, $N = 100$ and $\Delta p = 0.49505$. Since the system visits all the states with almost the same frequency, in this case, a flattened shell appears to be filled up, around the bisecting line. Obtained from Fig. 9 of [1].

that is the time average of the state of the system relative to the molecule i, during the time interval $[0,+\infty\rangle$. (In this calculation, p is kept fixed, while $\forall i = 1,\ldots,L$, Δp_i is the realization of a normally distributed random variable with mean $\overline{\Delta p}$ and variance σ^2. The discrete time variable j is indicated with t for the sake of clarity. This notation change will be used throughout in the following.)

Then we have computed the ensemble expectation of the time average of the state of the system formed by all the L molecules, during the time interval $[0,+\infty\rangle$:

$$\langle X\rangle_{\Delta p} = \frac{1}{L}\sum_{i=1}^{L}\bar{X}_i = \frac{1}{L}\sum_{i=1}^{L}\left(\lim_{T\to\infty}\frac{1}{T}\sum_{t=1}^{T}X_i(t)\right) \tag{14}$$

In Fig. 3, the quantity $(1/N)\langle X\rangle_{\Delta p}$ is plotted as a function of $p \in [0,1]$, corresponding to several values of $\overline{\Delta p}$; $\forall i = 1,\ldots,L$ Δp_i is randomly distributed according to a Gaussian with mean $\overline{\Delta p}$ and variance σ^2.

Alternatively, we have computed

$$\bar{X}_{\Delta p} = \lim_{T\to\infty}\frac{1}{T}\sum_{t=1}^{T}X[t,\Delta p(t)] \tag{15}$$

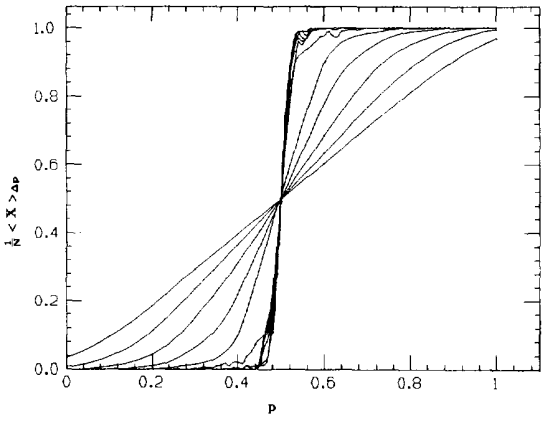

Fig. 3. Plot of the normalized ensemble and time average $(1/N)\langle X\rangle_{\Delta p}$ as a function of $p \in [0,1]$, in correspondence with increasing values of $\overline{\Delta p}$ from 0 to 1; Δp is randomly distributed according to a Gaussian with mean $\overline{\Delta p}$ and standard deviation $\sigma = 0.1$ Here the simulation has been made by using the MC obtained by Eq. 12 (see Section 3), $L = 1000$ and the approximation to the limit $\bar{X}$ has been computed for $T = 1000$ iterations.

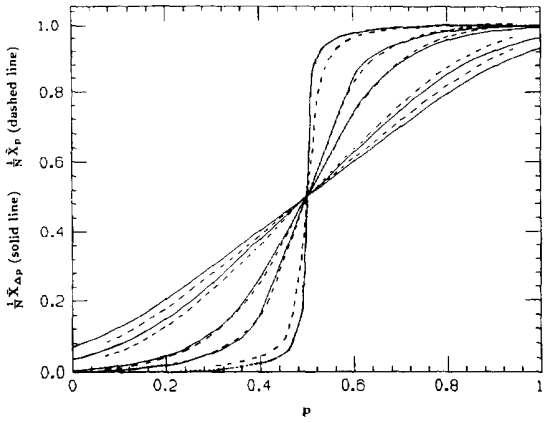

Fig. 4. Plot of $(1/N)\bar{X}_{\Delta p}$ as a function of $p \in [0,1]$, in correspondence with increasing values of $\overline{\Delta p}$ from 0. to 0.8 (solid lines); Δp is randomly distributed according to a Gaussian with mean $\overline{\Delta p}$ and standard deviation $\sigma = 0.2$. Plot of $(1/N)\bar{X}_p$ as a function of $p \in [0,1]$, in correspondence with increasing values of $\bar{p}$ from 0. to 0.8 (dashed lines); p is randomly distributed according to a Gaussian with mean $\bar{p}$ and standard deviation $\sigma = 0.2$ Here the simulation has been made by means of the MC obtained by Eq. 12 and the approximation to the limit $\bar{X}$ has been computed for $T = 10000$ iterations.

that is the time average of the state of the system relative to one molecule extracted from the considered ensemble, supposing to maintain p fixed and letting $\Delta p = \Delta p(t)$ vary, at any time t of simulation, according to a Gaussian $\mathcal{N}(\overline{\Delta p},\sigma^2)$. We have also computed

$$\bar{X}_p = \lim_{T\to\infty}\frac{1}{T}\sum_{t=1}^{T}X[t,p(t)] \tag{16}$$

that is the time average of the state of the system relative to one molecule extracted from the considered ensemble, for Δp fixed and variable p, at any time t of simulation, according to a Gaussian variable with mean $\bar{p}$ and variance σ^2.

In Fig. 4, $(1/N)\bar{X}_{\Delta p}$ is plotted as a function of $p \in [0,1]$, in correspondence with several values of $\overline{\Delta p}$ (solid lines); Δp is randomly distributed according to a Gaussian with mean $\overline{\Delta p}$ and variance σ^2. In the same figure, also $(1/N)\bar{X}_p$ is plotted as a function of p, in correspondence with several values of Δp, where p is Gaussian with mean $\bar{p}$ and variance σ^2 (dashed lines).

In Figs. 3 and 4, the curves assume a sigmoidal shape. Moreover, the curves related to the double

expectation $\langle X \rangle_{\Delta p}$ and to the time average $\bar{X}_{\Delta p}$, are qualitatively the same.

Thus, in order to save a lot of computation time for the simulation, we can suppose to compute the mean given by $\bar{X}_{\Delta p}$ instead of $\langle X \rangle_{\Delta p}$, obtaining the same qualitative results. For all figures, the approximation to the limit $\bar{X}$ has been calculated for $T = 10000$ iterations, while L has been taken equal to 1000.

Indeed, as far the data of the Fig. 4 are concerned, the computed value of $(1/N)\bar{X}_{\Delta p}$ as a function of $p = x \in [0,1]$ is fitted satisfactorily by the curve (see Fig. 5)

$$y = \frac{(2x)^{\alpha}}{1 + (2x)^{\alpha}} \tag{17}$$

By least square interpolation, we have found that also the exponent α turns out to be a sigmoidal function of $\overline{\Delta p}$ (see Fig. 6; in the caption to Fig. 6 the sigmoidal function is precisely indicated). Moreover, the shape of this function does not vary strongly with σ. From Fig. 6 it is possible to calculate the $\overline{\Delta p}$ value corresponding to a given α value (in the range 0–50). In this way we can apply our stochastic model to real cooperative transition in biology. We have selected three representative examples: oxygen binding to haemoglobin (Fig. 7a), pH-induced helix–coil transition in polylysine (Fig. 7b) and thermal phase transition in DPPC vesicles (Fig. 7c). In each case, the transition was fitted with a general sigmoid:

$$y = A + \frac{(B - A)\, x^{D}}{C^{D} + x^{D}} \tag{18}$$

The fitting values used for each parameter are reported in the figure captions. The fitting was performed using a standard numerical fitting program based on the Marquardt algorithm. The function in Eq. 18 can be transformed into Eq. 17 by an appropriate change of variables. In the case of Fig. 7c, a further change of variables has to be applied to reverse the curve, i.e. to change it into its symmetric one with respect to the value C. Notice that the exponents α in Eq. 17 and D in Eq. 18 are proportional to the slope of the tangent lines to the curves at the middle point of transition. However, as can easily be seen, in the cases of Fig. 7a and b, the D value in Eq. 18 is equal to the α value in Eq. 17, while in Fig. 7c, $\alpha = -D$.

By inverting the sigmoidal function $\alpha = \alpha(\overline{\Delta p})$

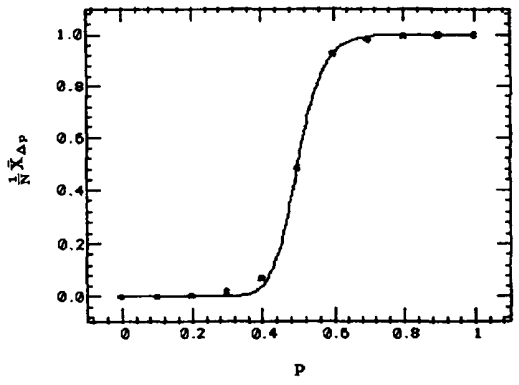

Fig. 5. Example of fitting $(1/N)\bar{X}_{\Delta p}$ by the curve given in Eq. 17, with $\sigma = 0.1$, $\overline{\Delta p} = 0.5$, $\alpha = 28$. (On the horizontal axes p, on the vertical one $(1/N)\bar{X}_{\Delta p}$.)

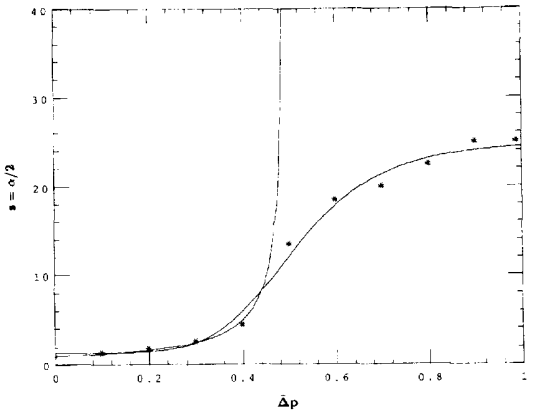

Fig. 6. Plot of the exponent α as a function of $\overline{\Delta p}$, where α is the exponent in Eq. 17, for the sigmoids relative to $(1/N)\langle X \rangle$ (on the horizontal axes $\overline{\Delta p}$, on the vertical one $s = \alpha/2$). Indeed, $s(\alpha)$ is the slope of the tangent line to the curve $\alpha = \alpha(\overline{\Delta p})$, at $\overline{\Delta p} = 1/2$. Here $\sigma = 0.1$, but the results does not vary appreciably with σ. The values obtained by computer simulation are marked with *; they are fitted by the sigmoid of equation $s = A + [(B - A)\overline{\Delta p}^{D}]/[C^{D} + \overline{\Delta p}^{D}]$, where $A = 1.38$, $B = 25$, $C = 0.516$ and $D = 5.58$. Also plotted is the curve $1/(1 - 2\overline{\Delta p})$, that is the slope of the lines given by $\bar{X}/N$ in Eq. 10, which represent the theoretical estimates in the case of constrained values of $p \in [\Delta p, 1 - \Delta p]$, with no distribution of Δp. For $\overline{\Delta p}$ small enough, as one expects, the latter curve agrees well with the one of $s(\overline{\Delta p})$.

which gives α as a function of $\overline{\Delta p}$ (see the caption to the Fig. 6, where this function is precisely indicated), once the value of $|D| = \alpha$ is known for each of the three selected cooperative transitions, the corresponding values of $\overline{\Delta p}$ can be found. The $\overline{\Delta p}$ values obtained in such a way are also indicated in the figure captions.

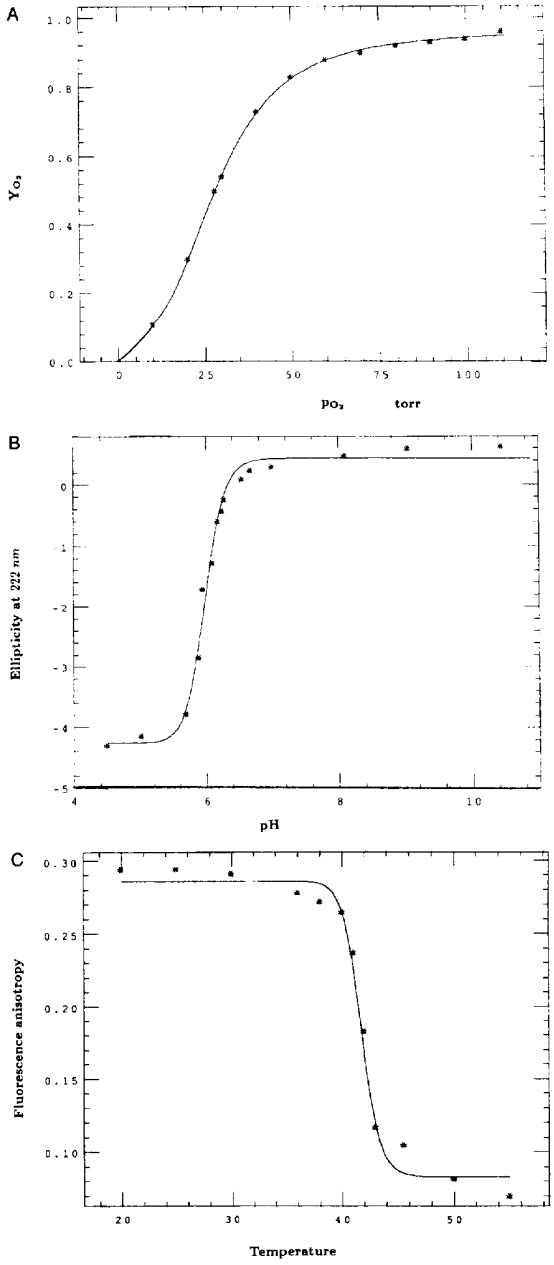

4. Analysis of sigmoidal-like simulations

In the preceding sections we have considered a model for cooperative interactions in macromolecules characterized by two parameters, p and Δp, one of which, Δp, measures the degree of cooperativity of the system. Indeed, the time average of the state of the system in an infinite time interval gives rise to a sigmoidal-like curve, when plotted as a function of p, and the greater the value of Δp, the more cooperative is the system, i.e. the steeper the sigmoidal behaviour.

Thus, we can say that the parameter Δp is not only a measure of the cooperativity of the system, but it also gives information about the complexity of the system.

In this section, we shall deal with general sigmoidal-like phenomena obtained by computer simulation and, in order to measure the complexity of a system, we introduce the so-called fractal dimension.

We recall that the fractal dimension (of covering) of a set E embedded in R^d is defined by (see [5]):

$$D = \lim_{r \to 0+} \{[\ln N(r)]/[\ln(1/r)]\} \qquad (19)$$

Fig. 7. (A) Oxygen dissociation curve (marked with *) of Hb in whole blood; on the horizontal axes the pressure p_{O_2}, on the vertical one Y_{O_2} (data obtained from [13]). The curve has been fitted with the sigmoid $y = A + [(B - A)x^D]/[C^D + x^D]$, with $A = 0.078$, $B = 0.961$, $C = 1.459$ and $D = 3.066$. By inverting the sigmoid function $\alpha = \alpha(\overline{\Delta p})$ (see the caption to Fig. 9), we get that an haemoglobine-like curve can be obtained with our model, taking $\overline{\Delta p} = 0.2013$. (B) Helix–coil transition in polylysine; on the horizontal axes pH, on the vertical one ellipticity at 222 μm (the data, marked with *, are obtained from [4]). The curve has been fitted with a sigmoid in which $A = -4.26$, $B = 0.437$, $C = 0.777$ and $D = 39.88$. By inverting the sigmoid function $\alpha = \alpha(\overline{\Delta p})$, we obtain the value $\overline{\Delta p} = 0.6513$. (C) Phase thermal transition in DPCC vesicles; on the horizontal axes the temperature, on the vertical one the fluorescence anisotropy (the data, marked with *, are obtained from [14]). The curve has been fitted with the sigmoid in which $A = 0.083$, $B = 0.2859$, $C = 1.62$ and $D = -41.89$. By inverting the sigmoid function $\alpha = \alpha(\overline{\Delta p})$, we obtain the value $\overline{\Delta p} = 0.68$. Then, we can observe an increase in the cooperativity degree from the case of Fig. 7a to the one of Fig. 7c.

where $N(r)$ is the number of d-cubes of side r which cover the set E.

We have dealt with some simulation runs of sigmoidal-like transition and we have computed the fractal dimension of a certain set of trajectories obtained during the simulation.

Of course, the fractal dimension of any trajectory obtained by computer simulation is zero, being a discrete set. However, by computing the quantity in Eq. 19 for r small enough, but not infinitesimal, one can obtain non-trivial qualitative information on the nature of the trajectory. This information is given by a number which we call fractal dimension (see also [1]).

We recall from the Introduction that the sigmoidal-like phenomena are empirically characterized by transitions following the curve given by Eq. 1, where the power α is related to the degree of cooperativity of the change in y as a function of $x \geq 0$. However, in cooperative phenomena, the variable x is not purely deterministic. We can suppose that it varies according to a Gaussian distribution with mean value $m = \bar{x} > 0$ and variance σ^2. By introducing an indetermination on the variable x, our aim is to characterize the fluctuations of y, as a function of x and α. For several values of m, σ and α, we have numerically obtained samples of points $\{x_j\}$ distributed according to $\mathcal{N}(m,\sigma^2)$, and then we have computed y_j by means of Eq. 1. Thus we have obtained a set of points $\{y_j\}$ from the interval [0,1]. In Fig. 8 two examples are reported for a Gaussian with $m = 1$, $\sigma = 0.6$ and two different values of α.

For instance, by considering the deterministic transition given by $x \to x/(1+x)$ for $x = m = 1$, we obtain the transition $1 \to 1/2$. By introducing a random fluctuation about x, according to a normal distribution, we do not obtain exactly the value $1/2$, but a different value, and the larger the dispersion (i.e. the larger is σ), the more this value deviates from $1/2$. Repeating the procedure, we obtain, for small values of σ, a set of values $\{y_j\}$ which lie approximately near the line $y = 1/2$ in a plot of y versus j; j can be interpreted as the time, and the number $\{x_j\}$ as the values (around the mean value m) assumed by the state-variable of the system at successive time intervals.

It is easily understood that, for large values of σ and α being large, the points $\{y_j\}$ obtained in the way described above are widely spread in the interval [0,1]. Interpreting these points as an orbit, this orbit appears to be dense in the interval [0,1].

We have computed the fractal dimension of the orbits obtained in this way, by means of Eq. 19, and we have related it to the cooperativity α of the system, as a function of m and σ. As expected, when the orbits appear to be dense in the unit

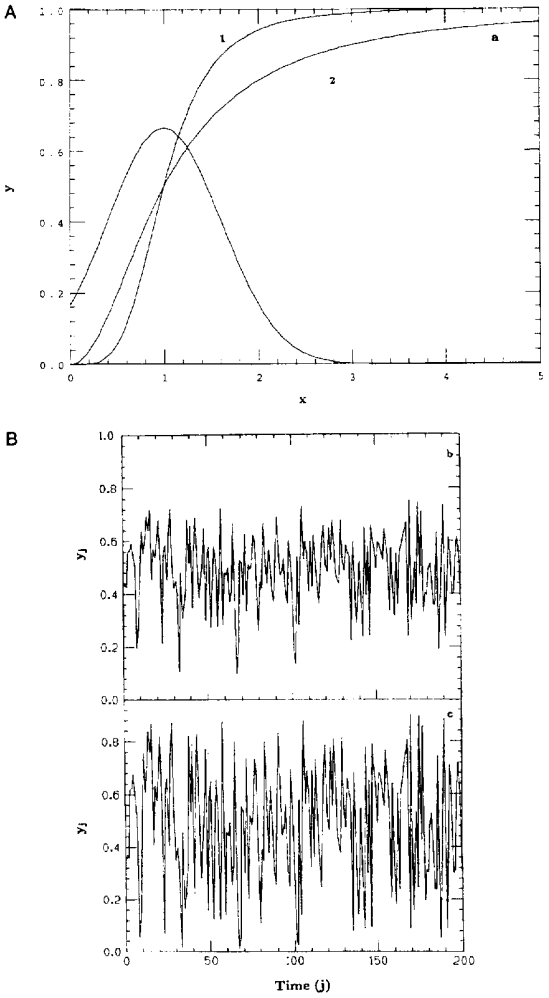

Fig. 8. Panel a: graphs of the Gaussian density ($m = 1$, $\sigma = 0.6$) and of the sigmoid curves given by Eq. 1 as function of x, for $\alpha = 4$ (1) and $\alpha = 2$ (2); panels b and c: plots of points $\{y_j\}$ from the interval [0,1] (trajectory) as a function of time j obtained by using Eq. 1, where the points $\{x_j\}$ are sampled at successive instants j from a Gaussian with $m = 1$ and $\sigma = 0.6$ for $\alpha = 2$ (b) and $\alpha = 4$ (c).

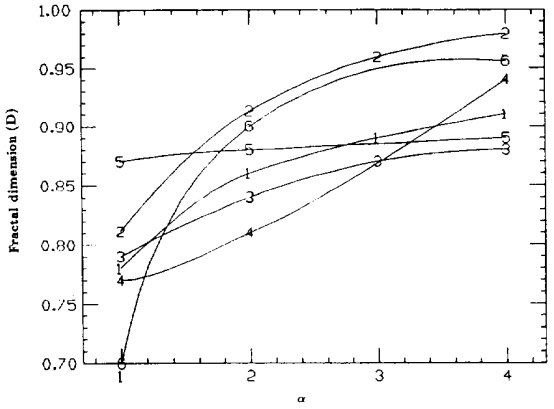

Fig. 9. Plot of the fractal dimension D (vertical axes) of the set $\{y_j\} \in [0,1]$ obtained by sampling $\{x_j\}$ according to a normal distribution and then applying the sigmoidal function $y = x^\alpha/(1 + x^\alpha)$, for several values of α from 1 to 4 (horizontal axes). The various curves refer to different values of the mean value m and of the standard deviation σ of the normal distribution. Precisely, the curve denoted with 1 refers to the case when $m = 1$ and $\sigma = 0.3$; the curve 2 refers to $m = 1$ and $\sigma = 0.6$; the curve 3 refers to $m = 1.25$ and $\sigma = 0.3$; the curve 4 refers to $m = 1.25$ and $\sigma = 0.6$; the curve 5 refers to $m = 0.75$ and $\sigma = 0.3$; the curve 6 refers to $m = 0.75$ and $\sigma = 0.6$. The fractal dimension D takes the maximum for $\alpha = 4$ and $m = 1$, $\sigma = 0.6$ (curve 2). In this case the set of points $\{y_j\}$ appears to be dense in [0,1].

interval, the fractal dimension reaches a maximum (Fig. 9), showing the greatest degree of cooperativity (that is complexity, in some sense) of the system.

5. Conclusions

Our stochastic model requiring only two parameters p, the mean probability, and Δp, the coupling capacity, can account for the main feature of cooperative transitions. In fact the simulated behaviour shows a transition which becomes more and more cooperative with increasing Δp value. Thus Δp corresponds to the degree of cooperativity of the system, while p relates to the independent value of the transition. The simulated transitions with fixed values of Δp and p do not show sigmoidal behaviour but have a linear shape (Fig. 1).

A sigmoidal pattern is instead obtained by introducing distributions in Δp (or p), which in the protein folding example, correspond to conformational distributions (Figs. 3 and 4). A sigmoidal-like relation between Δp and α has been established (Fig. 6).

A further outcome of this study concerns the noise of the dependent variable y at the midpoint of the transition ($x_{1/2}$). We observe that the width of the noise increases with the exponent α of the sigmoid (Fig. 8). This phenomenon was already reported by Weber [12] in a paper concerning a simulation of the conformational drift in oligomeric proteins. The frequencies of the y values obtained with a random fluctuation of x around $x_{1/2}$ is approximately a Gaussian at low α values, but flattens as α increases and at high enough α values becomes concave, as the contributions from the extreme values of y are predominant (Fig. 10).

Finally, we have introduced a new measure of the y-noise, in the fractal dimension of the time trajectories of $y(t)$. The results obtained with the simulated data show that the fractal dimension increases (from 0 to almost 1) along with α, suggesting that the cooperativity can be evaluated by means of the fractal dimension of the noise.

All numerical computations and simulations have been executed by means of a VAX 8600 Computer

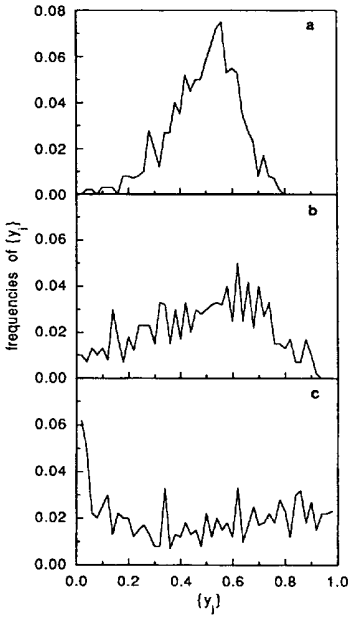

Fig. 10. Plots of the frequencies of $\{y_j\}$ for $m = 1$, $\sigma = 0.6$ and $\alpha = 2$ (a), $\alpha = 4$ (b) and $\alpha = 8$ (c) (see also Fig. 9).

at the Department of Mathematics, the University of Rome "Tor Vergata".

References

[1] M. Abundo, L. Accardi and N. Rosato, Math. Models Methods Appl. Sci., 6(5) (1995) in press.
[2] E. Antonini and M. Brunori, Hemoglobin and Myoglobin in their Reactions with Ligands, North Holland, Amsterdam, 1971.
[3] D. Chapman, Quart. Rev. Biophys., 8 (1975) 185.
[4] Y.P. Myer, Macromolecules, 2 (1969) 624.
[5] B.B. Mandelbrot, Fractals, Form, Chance and Dimension, Freeman, San Francisco, CA, 1977.
[6] C.L. Webber and J.P. Zbilut, J. Appl. Physiol., 76 (1994) 965.
[7] B. Hess and M. Markus, Trends Biochem. Sci., 12 (1987) 45.
[8] B.J. West and A.L. Goldberger, Am. Sci., 75 (1987) 354.
[9] A. Ansari, S. Berendzen, S.F. Bowne, H. Frauenfelder, I.E. Iben, T.B. Sanke, E. Shymsunder and R. Young, Proc. Natl. Acad. Sci. USA, 82 (1985) 5000.
[10] R. Alcala, E. Gratton and F. Prendergast, Biophys. J., 51 (1987) 597.
[11] G. Mei, N. Rosato, N. Silva, R. Rusch, E. Gratton, I. Savini and A. Finazzi Agró, Biochemistry, 31 (1992) 7224.
[12] G. Weber, J. Mol. Liq., 42 (1989) 255.
[13] D. Voet and J.G. Voet, Biochemistry, Wiley, New York, 1990, p. 213.
[14] M. Shinitzky and Y. Barenholz, Biochem. Biophys. Acta, 515 (1978) 367.